Ocean Dynamics (2012) 62:1043–1057
DOI 10.1007/s10236-012-0545-5

Extreme flows and unusual water levels near a Caribbean coral reef: was this a case of a "perfect storm"?

Tal Ezer · William D. Heyman · Chris Houser · Björn Kjerfve

Received: 11 July 2011 / Accepted: 10 April 2012 / Published online: 9 May 2012

Abstract Observations of currents aimed to study the flow near a spawning aggregation reef, Gladden Spit off the coast of Belize, reveal unusually strong currents on 19–20 October 2009 (the current speed was over 1 ms^{-1}, when the mean and standard deviation are 0.2 ± 0.12 ms^{-1}). During this short time, the water level was raised by 60–70 cm above normal in one place, but lowered by 10–20 cm in another location just 2 km away. The temperature dropped by over 2°C within a few hours. Analyses of local and remote sensing data suggest that a rare combination of an offshore Caribbean cyclonic eddy, a short-lived local tropical storm, and a Spring tide, all occurred at the same time and creating a "perfect storm" condition that resulted in the unusual event. High-resolution simulations and momentum balance analysis demonstrate how the unique shape of the coral reef amplified the coastal current through nonlinear flow–topography interactions. The suggested mechanism for the water level change is different than the classical wind-driven storm surge process. The study has implications for the influence of external forcing on mixing processes and physical–biological interactions near coral reefs.

Keywords Numerical model · Caribbean coral reef · Storm surge · Flow–topography interaction

Responsible Editor: Leo Oey

This article is part of the Topical Collection on the *3rd International Workshop on Modelling the Ocean 2011*

T. Ezer (✉)
Old Dominion University,
Norfolk, VA, USA
e-mail: tezer@odu.edu

W. D. Heyman · C. Houser
Texas A&M University,
College Station, TX, USA

W. D. Heyman
e-mail: wheyman@geog.tamu.edu

C. Houser
e-mail: chouser@geog.tamu.edu

B. Kjerfve
World Maritime University,
Malmö, Sweden

B. Kjerfve
e-mail: kjerfve@wmu.se

1 Introduction

The Mesoamerican Barrier Reef System in the western Caribbean Sea stretches along the coasts of Mexico, Belize, Guatemala, and Honduras (Fig. 1a) and serves as an essential source of marine biodiversity and productivity for the region (Miloslavich et al. 2010). Studies of the Belize Barrier Reef identified spawning aggregation sites for many species of Caribbean fishes (Heyman et al. 2005, 2007, 2008; Heyman and Kjerfve 2008). Those spawning aggregation sites have a unique geomorphology with large horizontal curvatures and convex steep slopes (Heyman and Requena 2002; Kobara and Heyman 2008; Wright and Heyman 2008), suggesting that flow–topography interactions and intense mixing there help disperse larvae and eggs from these sites and then transport them into more protected areas (Ezer et al. 2011). The exact forcing mechanisms of small-scale flow variability (scales of a few meters to a few kilometers) in the vicinity of the reefs are not yet fully understood, though both remote forcing by Caribbean eddies (Ezer et al. 2005) and local variability by tides, winds, and internal waves may play a role (Ezer et al. 2011).

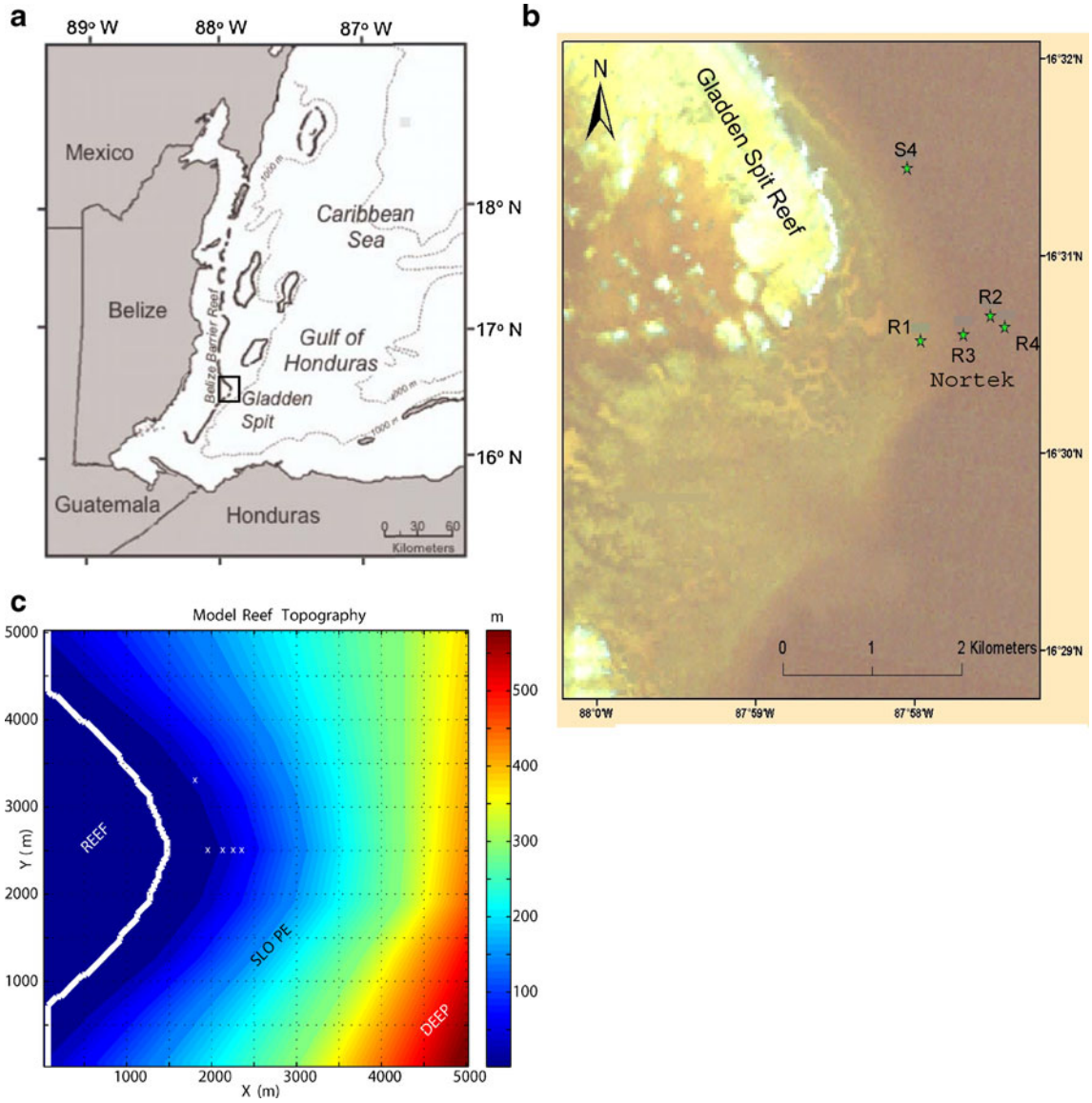

Fig. 1 **a** Map of the west Caribbean Sea region and the Gladden Spit reef. **b** Satellite image of Gladden Spit and the location of the observations used in this study. **c** The topography used by the numerical model. Temperature was recorded at four locations at depths of about 10 m (*R1*), 30 m (*R3*), 40 m (*R2*), and 50 m (*R4*). Bottom pressure was recorded at about 25 m depth at S4 and at R3. Velocity was recorded by a current meter at about 23 m at S4 and by Nortek (ADCP) profiler at R3. *Green stars* in **b** indicate the location of observations while white *X*s in **c** indicate the approximated location of the "instruments" in the model

The focus of our study is Gladden Spit Reef off Belize, where fish aggregation events have been studied extensively over recent years (Heyman et al. 2005, 2008), and where instruments have been deployed (Fig. 1b) to measure and monitor changes in temperatures and currents near this reef. Ezer et al. (2011) showed analysis and simulations of high-frequency oscillations in temperature and velocity during the major spawning period (May–June) that indicate the existence of internal waves and the amplification of flow variability due to the reef's unique topography. Nevertheless, the analysis also reveals unusual observed water level in October 2009 (see Fig. 3d in Ezer et al. 2011) that was assumed to be either an instrumental error or yet to be explained phenomenon. The passage of tropical storms and hurricanes across the western Caribbean Sea can produce strong currents and storm surges, as shown for example by the numerical simulations of Oey et al. (2006, 2007) and Sheng et al. (2007). However, the unusual water level signal observed on October 2009 was the largest recorded during the 2 years of available observations.

Figure 2 shows, for example, the changes in temperature on October 2009 at four locations near the center of the reef (see Fig. 1b for location). Until about 17 October, the temperature at 10 m depth shows daily variations, the

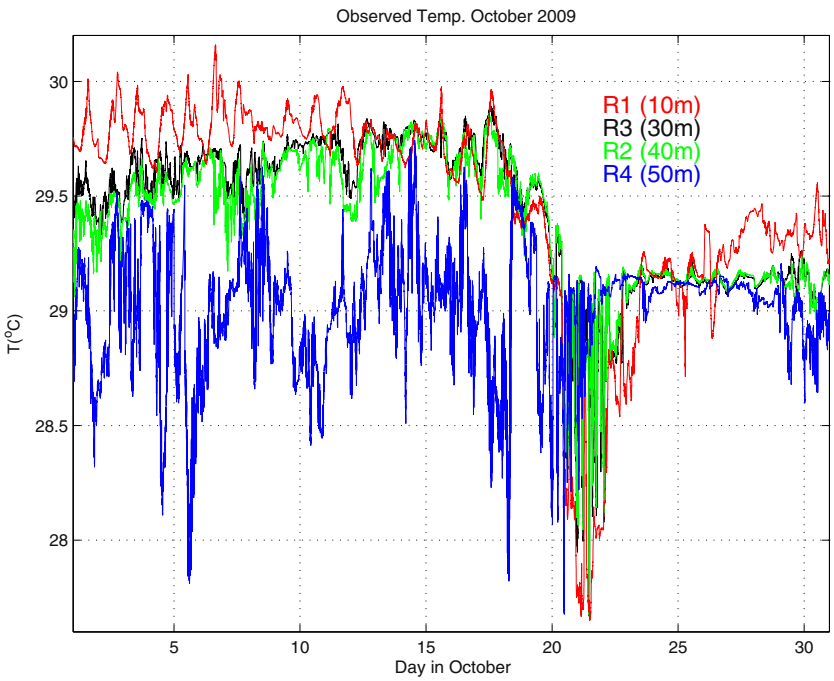

Fig. 2 Observed temperatures at the four sites (*R1–R4*) shown in Fig. 1b on October 2009. Measured interval is 1 min and the instrument depth (located just above the bottom) is indicated

temperatures between 30 and 40 m gradually warmed, and the temperature at 50 m shows high-frequency fluctuations of about 1–1.5°C; the latter are likely associated with internal waves as shown by Ezer et al. (2011). Between 17 and 21 October, the temperature in the upper 40 m drops by more than 2°C, and then, after considerable high-frequency fluctuations, the water settled at temperatures about 1°C colder than those observed before 17 October. By 24 October, the entire upper 50 m of the water column had almost the same temperature, indicating that a strong mixing event had occurred. The most common explanation for intense mixing in this region (as seen in Fig. 2) is the passage of hurricanes and tropical storms. For example, hurricane Wilma passed just north of the study area in 2005, making landfall on the Yucatan Peninsula before heading to Florida. Wilma reached a category 5 hurricane with winds up to 80 ms^{-1} and caused cooling of about 1°C in the Western Caribbean Sea as obtained from observations and models (Oey et al. 2006, 2007). Hurricane Mitch, also a category 5 hurricane with winds close to 80 ms^{-1}, made landfall in Honduras in 1998, approximately 200 km east southeast of our area of interest. Measurements, taken at Gladden Spit Reef during the passage of hurricane Mitch, show southeastward currents that intensified from ~0.1 to ~0.3 ms^{-1} and cooling of the water by about 1°C. The passage of hurricane Mitch also generated large changes in salinity over a vast area of the Gulf of Honduras due to the very large amount of precipitation associated with the hurricane (Sheng et al. 2007). As will be shown later, the measured currents on October 2009 were more than three times stronger than during the passage of hurricane Mitch, and to our knowledge, the largest ever recorded at Gladden Spit.

Detailed analysis of over 2 years of current meter data from the reef will be reported separately. This study focuses on a limited period, 17–21 October 2009, aiming to describe the unusual observations that occurred near the Gladden Spit reef during this time. Analysis of local and remote measurements, model results, and scale analysis will help us to better understand the dynamics involved, forcing mechanisms, and possibly an explanation for the unusual observations. The paper is organized as follows: first the large-scale atmospheric and Caribbean Sea conditions are described in Section 2, then local observations and model results are described in Sections 3 and 4, respectively, and finally, a simple scaling analysis and conclusions are offered in Sections 5 and 6, respectively.

2 Large-scale atmospheric conditions and the Caribbean circulation

Since there are currently no local meteorological observations at Gladden Spit, satellite-derived data are presented. The satellite image in Fig. 3 shows the National Weather Service outlook for 20 October 2009, showing two areas of atmospheric instability, one in the eastern tropical Atlantic and one in the western Caribbean Sea (southeast of the study area); the forecast indicated low probability that these disturbances will be developed into tropical storms. In fact, tropical storms have not been observed during the weeks prior or after 17–21 October, but a small disturbance is seen in the study area where the Caribbean instability (the circle near the number "1" in Fig. 3) and an Atlantic front (stretching

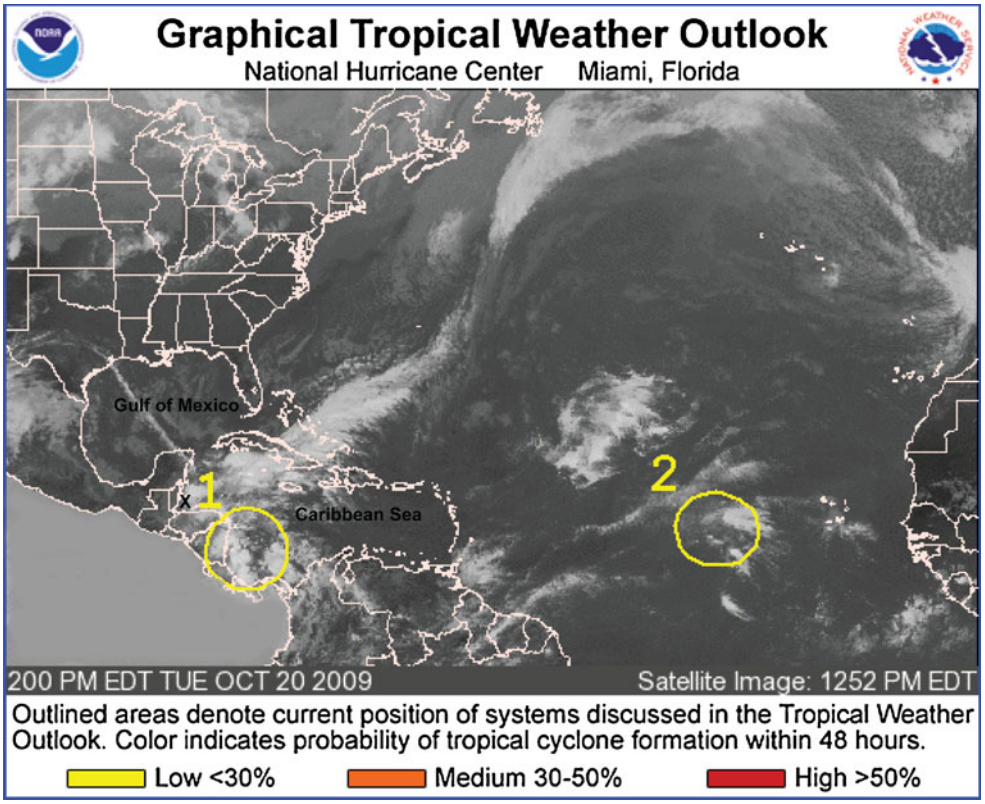

Fig. 3 The weather outlook from satellite image on 20 October 2009 indicates a weak front extending from the western Caribbean Sea to Newfoundland and 2 tropical disturbances (marked by *circles*) with low probability of developing into tropical storms. The area of our interest is the small disturbance noted by *X* northwest of disturbance number 1 where the Atlantic front and the Caribbean system intersect each other

from Belize to Newfoundland) intersect each other. Satellite-derived winds obtained from the QuikSCAT scatterometer data (at 25 km resolution) show how the seasonal easterly trade winds with wind speed less than 5 ms^{-1} before 17 October suddenly increased to 15–20 ms^{-1} with strong counter clockwise pattern during 19–20 October (Fig. 4). This short-lived local storm seen in the QuikSCAT data was not officially named as a tropical storm (which requires sustained winds over 17 ms^{-1} for an extended period of time).

Another potential source of forcing for currents near the reef is the remote impact due to variations in the Caribbean current and the propagation of Caribbean eddies. Ezer et al. (2005) show for example how mesoscale Caribbean eddies can reverse the predominantly southward flow near the Belize reef, and thus impact the dispersion of eggs from spawning aggregation sites (Heyman et al. 2008). Figure 5 displays the sea surface height (SSH), obtained from the gridded (0.25×0.25° resolution) AVISO satellite altimeter data (Ducet et al. 2000), in the weeks prior to the 17–21 October event. About a month before the storm, the Caribbean current was about 100–150 km northeast of the Gladden reef with its flow turning from southwestward to northeastward and a cyclonic (anticlockwise rotation) eddy is seen about 200 km east of the reef (Fig. 5a). During the following 2 weeks, the eddy moved westward into the Gulf of Honduras (Fig. 5b), and eventually by 14 October, most of the Belize reef had lower than normal SSH (Fig. 5c). While it is recognized that altimeter data are less accurate near the coast than in deep waters, geostrophic velocity calculations in this area based on the AVISO data do indicated anomalous southward flow of ~0.3 ms^{-1}, which is consistent with the expected influence of the eddy. The decreased offshore SSH in mid-October can also be seen in Fig. 6a (month 10.3–10.6).

3 Local observations near Gladden Spit reef

Measurements of near-bottom water temperatures were taken with four RBR instruments, deployed along a transect from the shelf edge to the reef edge, at depths of about 10, 30, 40, and 50 m (see Fig. 1b for locations and Fig. 2 for data). These locations at the tip of the reef are in the vicinity of the spawning aggregation sites that have been observed year after year (Heyman and Kjerfve 2008). Temperature records in 1-min intervals were used to identify internal waves in the study of Ezer et al. (2011). Currents were measured at two locations, one ("S4" in Fig. 1b) on the shelf edge at about 2 km north of the spawning site and the second one ("Nortek") at the R3 mooring near the tip of the reef. The first instrument is an InterOcean S4 electromagnetic current meter moored a few meters above the bottom in depths of ~25 m, and the second is a Nortek current profiler (ADCP) bottom-mounted at a depth of ~23 m; the instruments measure current velocity profiles from a height of ~1.5 m above the bed to the surface at 10-min intervals. Analyzed here are data from the first deployment of

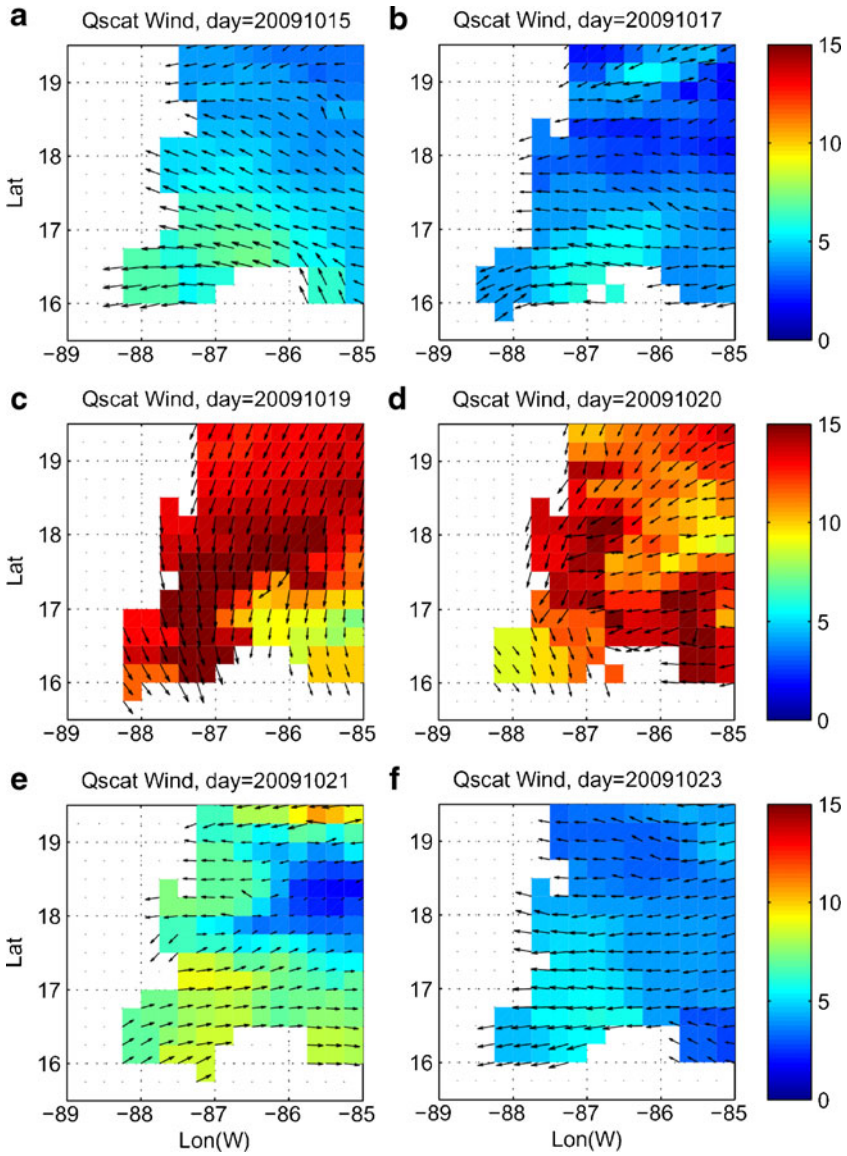

Fig. 4 **a**–**f** Satellite-derived QuikSCAT wind vectors and speed (in meters per second, in color), 15–23 October 2009

instruments, June to December 2009; the measurements continued in 2010 and 2011, but these longer observations will be analyzed in details in a follow-up paper.

Figure 6a shows the altimeter sea level anomaly from June to November 2009, and Fig. 6b shows the local water level obtained from the pressure sensors at S4 and at Nortek (the mean of each time series has been shifted for clarity). It is very clear that an unusual water level changes have been observed in mid-October, so a zoom in during a 10-day period (15–25 October) is shown in Fig. 6c. The typical tides in this area are mixed mainly semidiurnal with relatively small amplitude of about 10 cm (Fig. 6b; see also Ezer et al. 2005). The unusual high water level at S4 around 19 October happened during a Spring Tide, but this alone cannot explain a sudden increase of 70 cm in water level. The minimum SSH in Fig. 6a happened around 17 October, suggesting possible influence by the eddy discussed before and shown in Fig. 5. Interestingly enough, while the water level at the two sites follow each other and the tidal cycle most of the time, during this unusual period, when water level at S4 *increases* by almost 70 cm, the water level at Nortek *decreases* and reaches about 20 cm below mean sea level near the end of the storm.

The cyclonic eddy (Fig. 5) and local tropical storm (Fig. 4) should impact the flow near the reef, so the current speeds at the two sites are shown in Fig. 7. The time of the unusual water level (Fig. 6) happened at the same time that unusually strong currents are observed. The peak current speed at Nortek during the October storm is more than 6 standard deviations above the mean speed in the upper 10 m (Fig. 7a, b) and over 4 standard deviations above the mean speed near the bottom (Fig. 7c, d). How rare are those

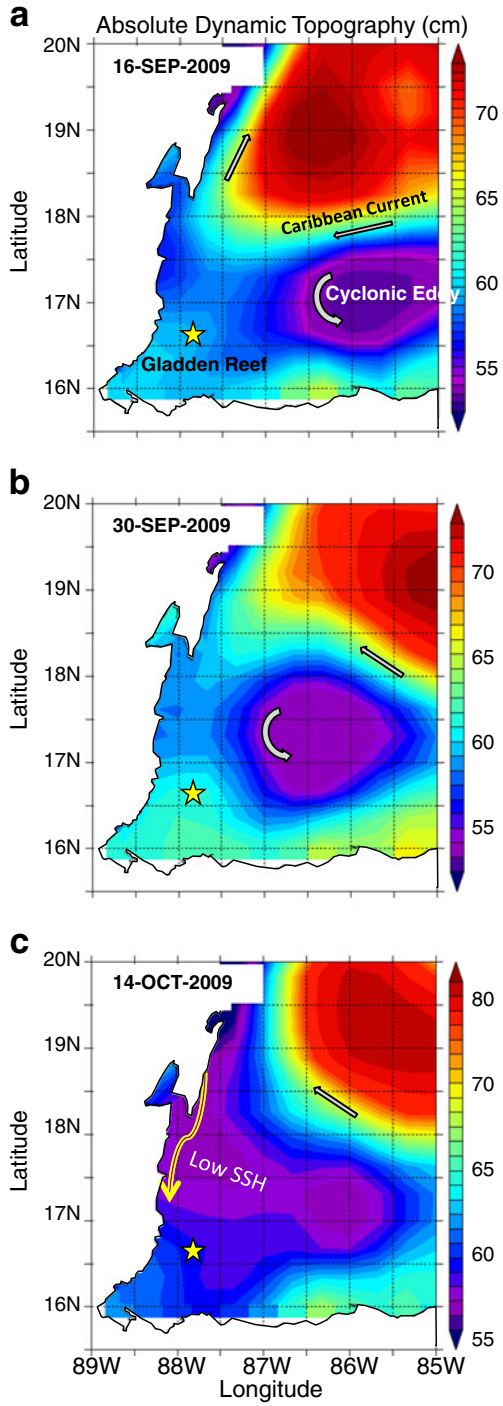

Fig. 5 **a**–**c** The absolute dynamic topography (sea surface height, *SSH*) obtained from AVISO satellite altimeter data in 2-week intervals. A schematic of the main current system is also shown. The location of the Gladden Spit reef is indicated by a *star*

events? For measurements taken at 10-min intervals, very rough estimates (assuming a normal distribution, which the currents are likely not obeying) show that currents larger than 4 standard deviations from the mean may occur about once every 4 months and currents larger than 6 standard deviations from the mean may occur only once every several years. The only measurements with velocities comparable in magnitude to those measured during the October storm were near the bottom at Nortek in mid-August and mid to late September 2009 (Fig. 7c). The large bottom currents there in August and September happened during times of relatively calm surface flows, indicating that they may have not been driven by overlying storms, but rather by topographically induced flows. In any case, analyses of many years of data are needed in order to have statistically significant estimate of the rarity of such strong flows and such a large sea level peak.

The surface current vectors and speeds observed by the ADCP at Nortek throughout the water column are shown in subpanels a and b Fig. 8, respectively. Strong southeastward flow persists for about 30 h with maximum flow over 1 m s^{-1}. The strong currents are almost barotropic for the top 20 m of the water column with flow decaying in the ~5 m above the bottom, as expected due to bottom friction. It is interesting to note that current measurements at Gladden Spit at 20 m depth during the passage of hurricane Mitch in October 1998 (Fig. 3 in Sheng et al. 2007) show intensifying flow with similar direction to that observed here, but the maximum water velocity during the 1998 hurricane was two to three times smaller than the velocity measured in October 2009 (Fig. 8a).

Previous studies (Heyman et al. 2008; Ezer et al. 2011) indicate that local winds may play only a minor role in driving local currents near the reef. Therefore, it is important to understand the mechanism in which local currents are driven by remote forcing such as the influence of the Caribbean current and Caribbean eddies. Regional models with 1–5 km resolution (Sheng and Tang 2004; Ezer et al. 2005; Tang et al. 2006) do indicate potential remote forcing (in particular, Ezer et al. 2005 show how eddies can reverse the coastal current), but they cannot simulate flows on scales of a few meters to hundreds of meters. There is an indication that a drop in sea level anomaly offshore (Fig. 6a) happened few days prior to the big local change in water level (Fig. 6b), but could this change drive the unusual local currents? To answer this question, geostrophic velocity anomaly along the coast (north–south direction) from the altimeter data is compared with daily averaged local velocity at S4 (Fig. 9). While small daily variations of offshore flow often do not seem to correlate with the local flow, when large changes occurred (likely due to eddies), there is a clear response by the local currents. In particular, during the ~6-month period, there were three cases of increasing southward large-scale flow (minimum below −0.1 ms^{-1}; red area in Fig. 9), in August, in October, and in November. In each of these cases, the southward flow was intensified (more negative in Fig. 9) at S4 about 2–5 days after the offshore change. In each of the three cases, altimeter data show a large cyclonic (counterclockwise rotating) eddy nearby. In 3

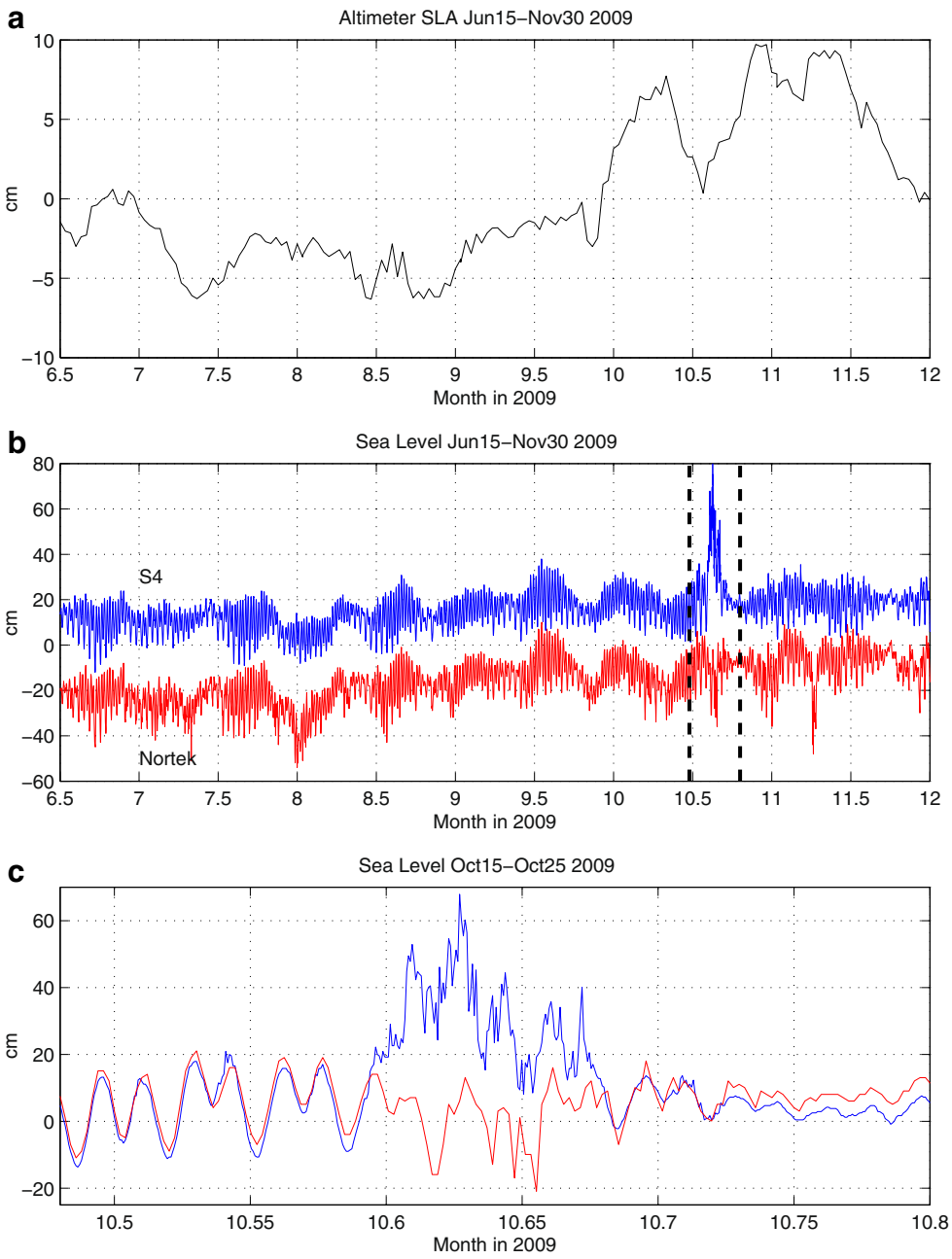

Fig. 6 **a** Daily sea level anomaly from satellite altimetry offshore Gladden Spit (88° W, 16.5° N) from June to November 2009. **b** Water level obtained from twice hourly bottom pressure records at S4 (*blue*, mean shifted by +15 cm) and Nortek (*red*, mean shifted by −15 cm). **c** The water level of **b** for the storm period, 15–25 October 2009 (highlighted by the *vertical dash lines* in **b**)

August and 16 November 16 (not shown), the cyclonic eddy remains northeast of Gladden (as in Fig. 5b), while in October 15, the eddy drifted all the way to the coast (Fig. 5c), creating larger response than in the other cases. The southward geostrophic flow increased by ~0.35 m s^{-1} during the 2 weeks prior to 15 October (red line in Fig. 9). Four days later, in 19 October, the local flow reached a maximum southward flow of ~0.35 ms^{-1} (blue line in Fig. 9). The linear regression correlation coefficient between the local and large-scale flow anomaly is about 0.15 with 95 % significance level, indicating that some portion of the local flow is driven by remote influence from the western Caribbean circulation.

4 High-resolution numerical ocean model simulations

The numerical ocean model used is the generalized coordinate, terrain-following ocean model (Mellor et al. 2002; Ezer and Mellor 2004) with an idealized topography of the reef as in Ezer et al. (2011). Idealized topography simulations with this model are useful for process studies of flow–topography interactions as done for example by Ezer (2005, 2006). The simple smooth bathymetry (Fig. 1c) resembles the general shape of the Gladden Spit Reef from 1 to 600 m depth. The purpose of the simulation is to conduct process and sensitivity studies. The domain size is a 5×5-km area, the horizontal grid cells are 50×50 m in size, and 21 vertical sigma layers

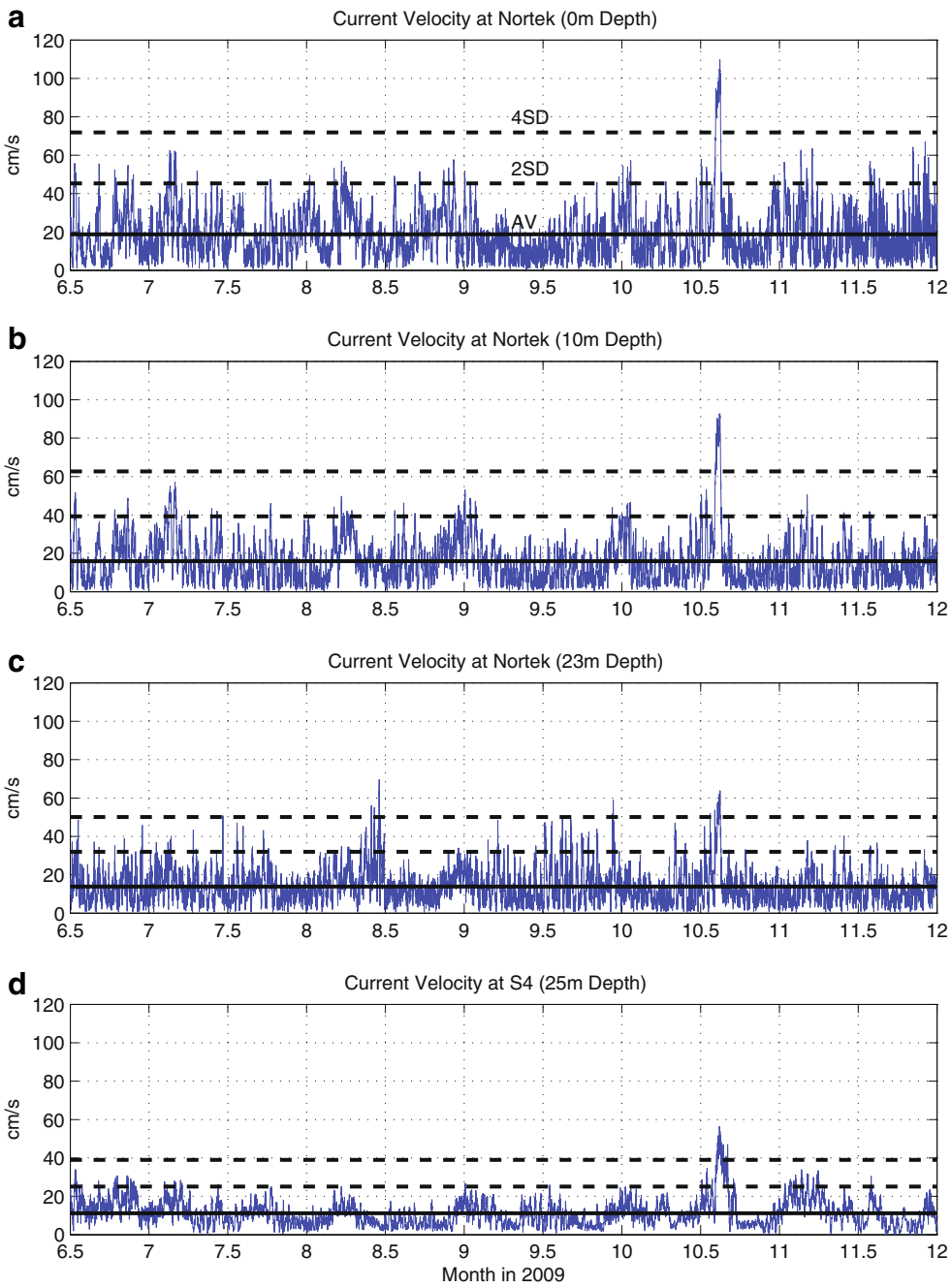

Fig. 7 Observed current speed from 15 June to 30 November 2009, at Nortek (**a**–**c**) and S4 (**d**). The average (*solid black line*) and 2 and 4 standard deviations (*dash lines*) are shown

evenly distributed between the bottom and surface are used. The model is forced by surface wind and southward flow imposed on the north boundary. The east and south open boundaries use radiation boundary conditions that allow flow and surface waves to enter or exit the domain with little disturbance. Surface heat and water fluxes are neglected for these short-term simulations. At present, there are almost no observations or realistic regional models of that area that can provide forcing data on scales of ~100 m to ~1 km. The only difference between the simulations of Ezer et al. (2011) and the experiments done here is that initial stratification, wind, and mean flow forcing are resembling the 17–21 October 2009 conditions. Five-day simulations after spin-up are described. In a model domain of that small size, the flushing time for replacing the entire volume of the model is only about 3 h, so there is no need for spin-up adjustment period of more than a few days. An idealized wind, resembling that in Fig. 4, is prescribed. Wind rotates counterclockwise and intensifies during the storm from 5 ms^{-1} westward in day 1 to 20 ms^{-1} southward at day 2.5 and then relaxes to 5 ms^{-1} eastward in day 5 (Fig. 10a). Another simulation without wind is also performed (i.e., currents are driven only by lateral inflow/outflow boundary conditions). The southward flow entering

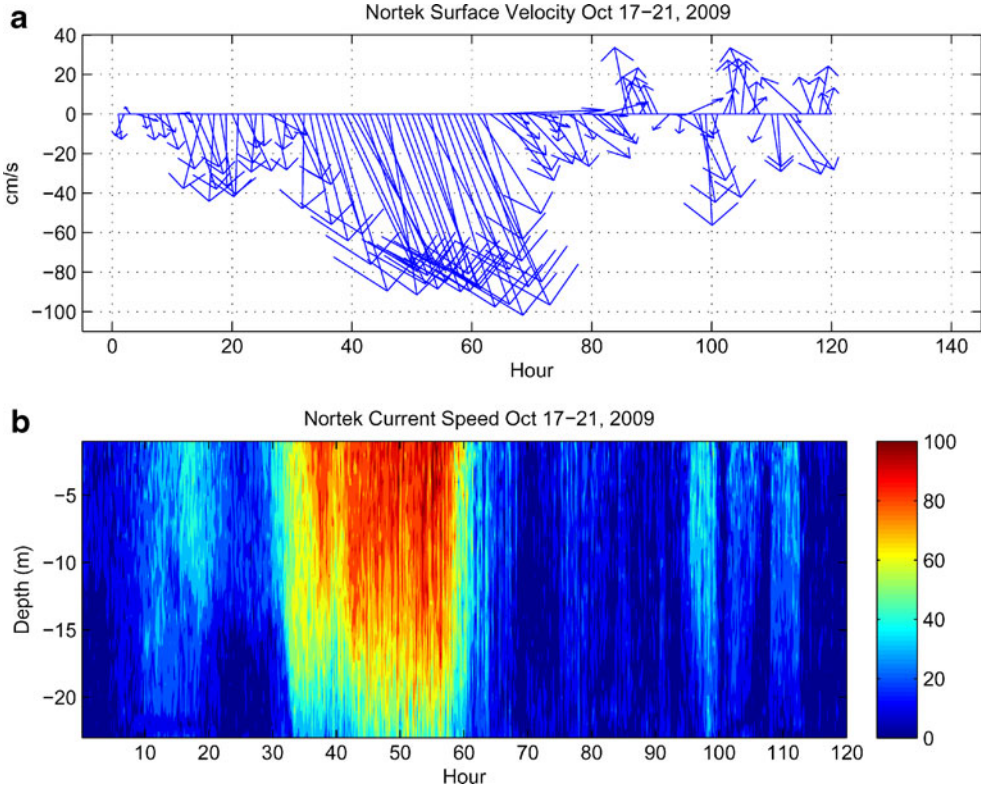

Fig. 8 Currents measured by ADCP at Nortek, 17–21 October 2009. **a** Hourly surface velocity vectors and **b** current velocity from the surface to 1.5 m above the bottom measured every 10 min

the model at its northern boundary (representing the large-scale flow) is set as a linear vertical velocity profile at the top 50 m of the model with an average speed that is proportional to the hourly current speed at S4 (S4 is located ~1.5 km south of the north boundary, Fig. 1c). It was empirically found that setting the maximum surface flow on the north boundary to 85 % of the observed speed at S4 reproduces the observed currents at S4 quite well (Fig. 10c); this is the only calibration made in the model. The slightly different velocity direction in the model (Fig. 10c) compared with the observations (Fig. 10b) is the result of the slightly different slope orientation in the model topography (Fig. 1c) compared with the real topography (Fig. 1b). Note that for building a realistic forecast system in this area, a more realistic wind forcing and a more

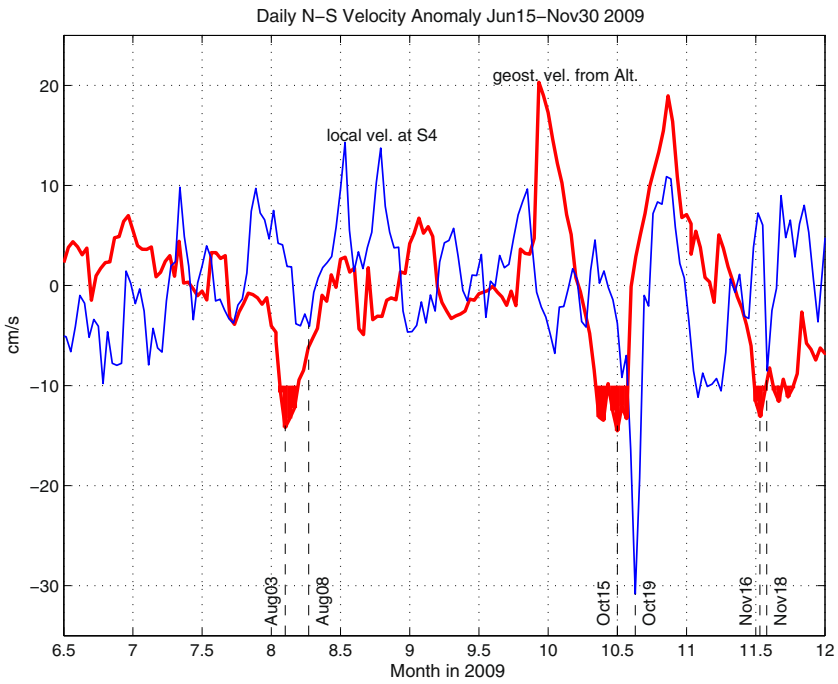

Fig. 9 The daily averaged anomaly of the north–south component of the local flow (*blue line*) and large-scale flow (*red line*). The local flow obtained from the S4 current meter at 25 m depth. The large-scale flow obtained from the geostrophic surface currents calculated from AVISO altimeter data at ~25×25 km box centered at 16.5° N, 88° W. *Filled red areas* represent three periods when the geostrophic velocity anomaly had minimum values below −10 cm s^{-1}; the days of those minima and corresponding minima in the local flow are indicated

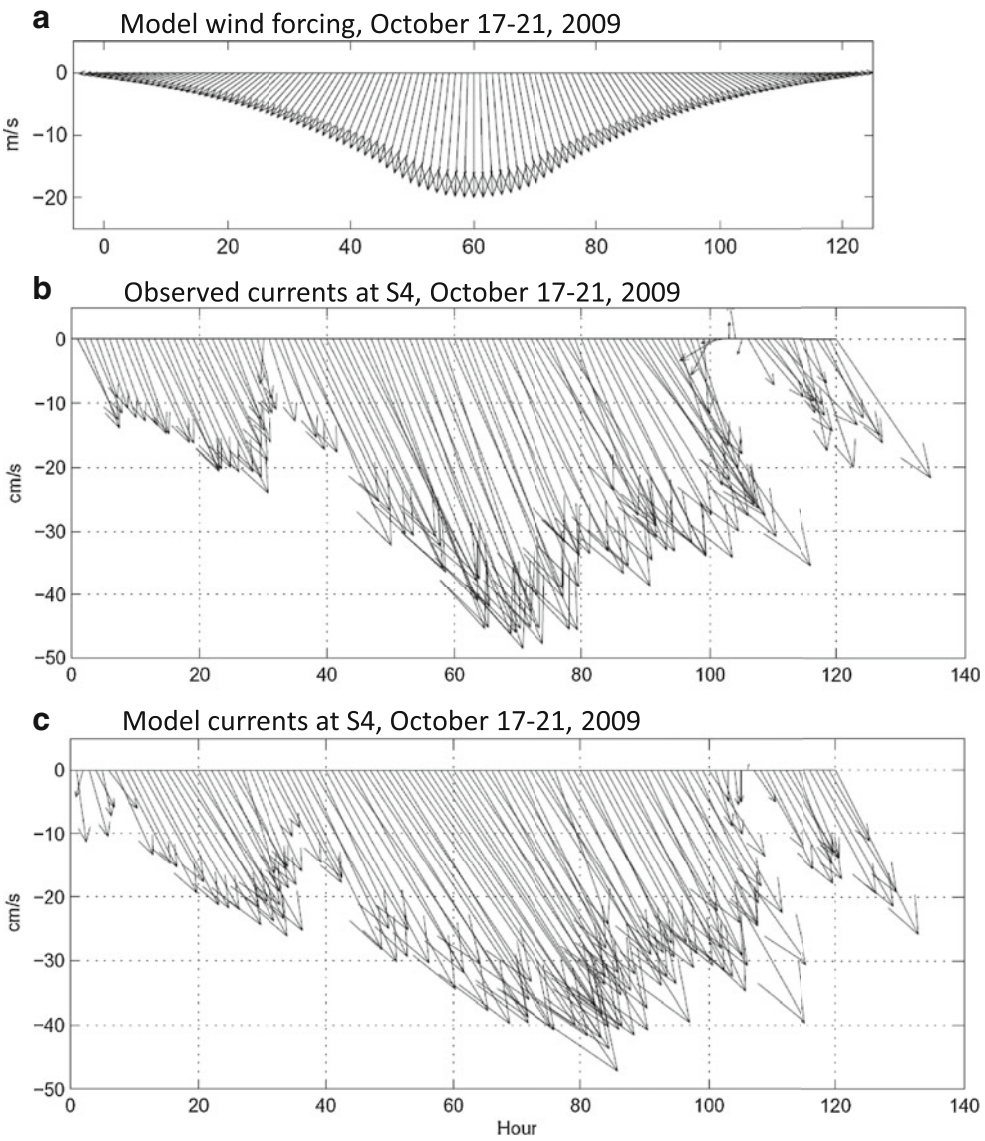

Fig. 10 **a** Hourly wind used as forcing in the model. **b** Hourly current meter observations at 25 m depth at S4 for 17–21 October 2009. **c** Same as **b**, but from the numerical ocean model simulations

accurate topography may be needed, while here the model is used primarily for process studies.

The simulated surface currents before, during, and after the storm are shown in Fig. 11. Before the storm, the typical wind in this region is easterly trade winds and the water flow is southward hugging the reef (Fig. 11a). The flow increases from ~0.1 to 0.2 ms^{-1} away from the reef to ~0.4 ms^{-1} near the tip of the reef (where spawning aggregations occur). When the wind and boundary flow increases during the storm, surface currents larger than 1 ms^{-1} are simulated near the tip of the reef up to a few hundred meters from the coast and velocities over 0.6 ms^{-1} can be seen some 2 km from the reef (Fig. 11b). The simulations without wind show somewhat weaker currents that do not extend as far offshore (Fig. 11e). The region most affected by the winds is the separation point of the current from the tip of the reef and the associated recirculation gyres in the lee side of the reef. The shape of the reef clearly intensifies the flow, a result of potential significance for dispersion of eggs from spawning sites (Ezer et al. 2011). After the storm has passed, a small clockwise recirculation gyre is seen in this area south of the reef (Fig. 11c); the recirculation gyre is more prominent in the simulation without winds. It should be clarified though that the "wind-forced" versus "no-wind" model comparisons only tests the impact of the local wind. The strong southward flow (even in the no-wind case), in fact, includes large-scale wind-driven effects on the coastal flow in the western Caribbean Sea (as well as eddy-driven influence). It is interesting to note that the recirculation gyres found here in the wake of the reef promontory would contribute to local retention of newly released gametes and eggs of fishes that spawn at Gladden Spit. This phenomenon of gyres, generated in the wake of capes or islands helping eggs and larvae settlement and retention, has been observed at other locations such as the

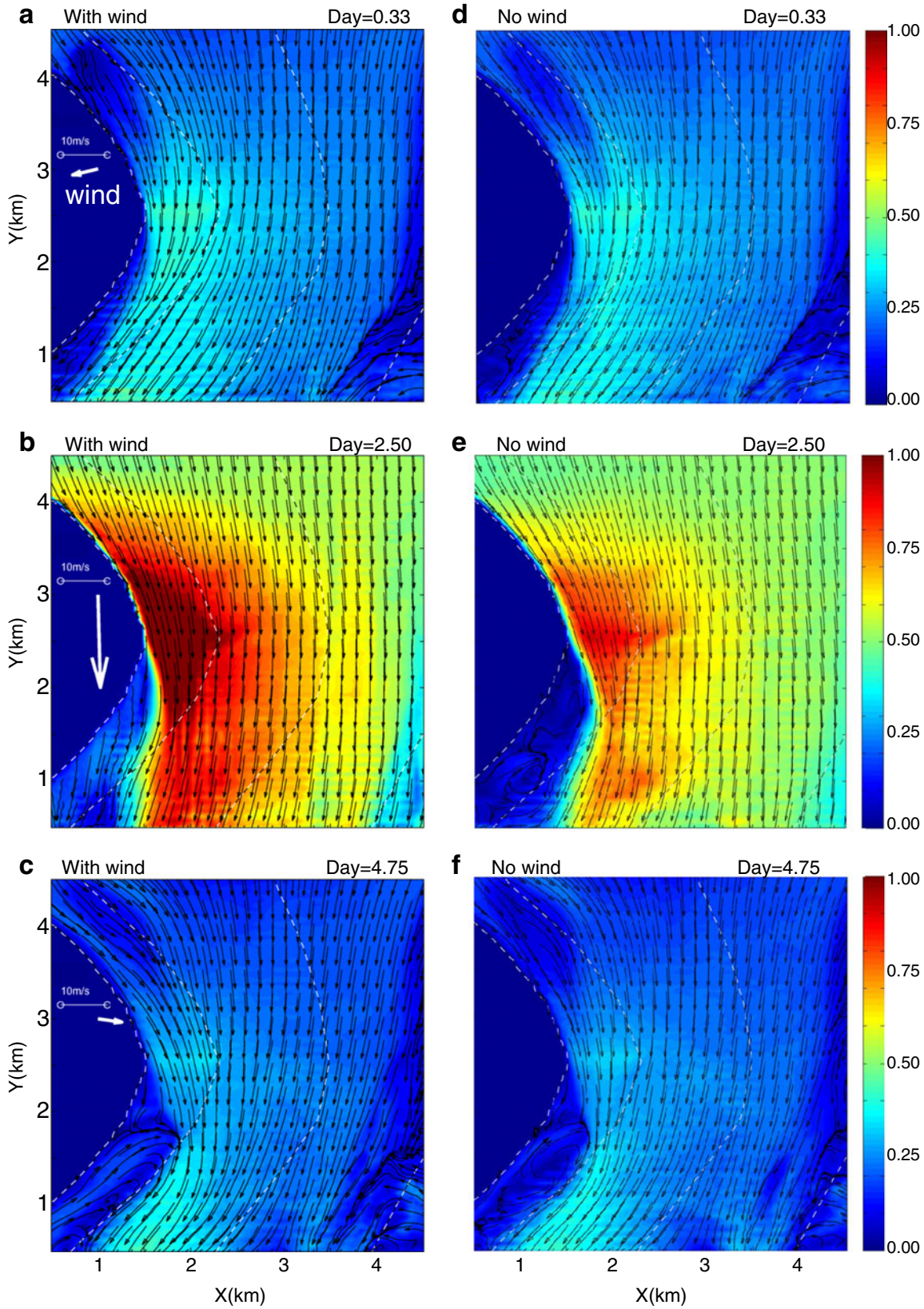

Fig. 11 Model-simulated surface velocity vectors and speed (in meters per second in color) for (top to bottom) ~2 days before the storm, during the peak of the storm, and ~2 days after the storm. Left panels (**a**–**c**) show the simulation with wind (*white arrows* show the wind vectors) and right panels (**d**–**f**) show the simulation without wind. *Dashed lines* show contours of the topography in the model (bottom depths of 5, 50, 200, and 400 m)

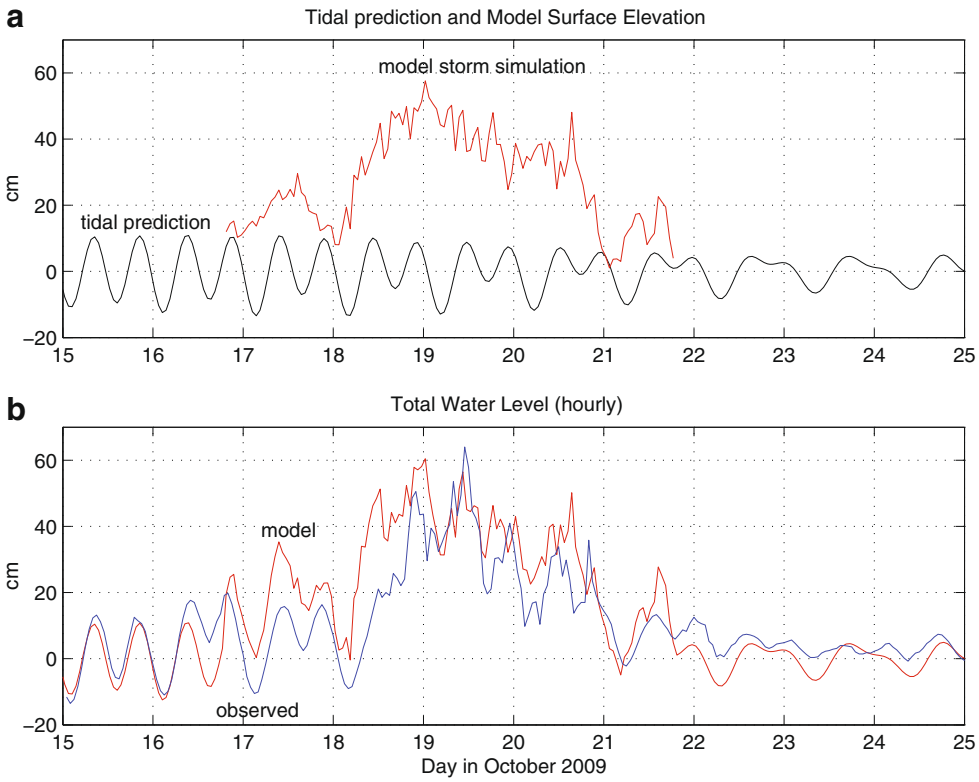

Fig. 12 **a** Tidal water level predicted from tidal constituents (*black line*) for 15–25 October 2009, and model surface elevation simulation near S4 (*red line*) for the storm period, 17–21 October 2009. **b** The total simulated water level of tides plus storm (*red line*) and the observed water level at S4 (*blue line*; same as the *blue line* in Fig. 6c, but hourly averaged)

Hawaiian Islands (Lobel and Robinson 1986) and the coast of California (Wing et al. 1998).

Can the unusually strong wind and eddy-driven flow explain the extreme observed water level rise in October, when water level was more than three times the highest tide measured (Fig. 6b)? Figure 12a compares the simulated water level change due to wind and large-scale flow with the tidal contribution; the tides are based on a separate prediction using six tidal constituents (given in Ezer et al. 2005). Note that the local wind impact on the simulated water level is very small so that simulated water level without local winds (not shown) are almost identical to Fig. 12a. The storm-driven (wind and large-scale flow) water level rise is about three times larger than the maximum high tide. The combined impact of the storm and tides in Fig. 12b is in a very good agreement with the observed signal at S4. At the beginning of the storm period, the mostly semidiurnal tide was at the Spring Tide period (with large amplitude), creating additional modulations of sea level and larger peaks, but by the end of the storm, a Neap Tide period started. The results demonstrate the fast changes experienced in this region, whereas a 4-day period of large variability in water level (Fig. 12b) and temperatures (Fig. 2), 18–21 October, is followed by a 4-day period of very weak currents and small variability, 22–25 October. This rapidly changing environment may have implications for the biological communities of the reef. The results suggest that the water level variations are the result of the combined effect of outside flow forcing and tidal variations and not due to the local wind (which in the model is simply a counterclockwise rotating smooth wind with no high-frequency variations, see Fig. 10a). This result does not imply that wind is unimportant, but that regional storms may act indirectly on the reef by modifying the along-reef coastal flow (which in our case is imposed on the model boundary). The lack of long-term accurate local wind measurements in this region prevents us from looking at the role of the wind in more details at this point. The model also simulated about 1°C cooling trend induced by the storm, but longer simulations with a more realistic model (including temperature observations away from the reef) are needed to simulate the details as seen in Fig. 2.

5 A simple dynamic explanation

So what is the prevailing dynamics that can create a water level gradient $(\Delta\eta/\Delta x)\sim$(1 m over 2 km) between S4 and Nortek (Fig. 6c)? For large-scale open ocean flows where geostrophic balance prevails, such sea level change would equivalent a geostrophic velocity of $V_g=(g/f)(\Delta\eta/\Delta x)\approx$ 122 ms^{-1}, where g and f are the gravitational constant and the Coriolis parameter ($f\sim4\times10^{-5}$ at 16° N), respectively. This velocity is of course unrealistic. For a spatial scale $L\sim$ 1 km and velocity $U\sim1$ ms^{-1}, the Rossby number $Ro=U/(fL)\approx25$, so that the Coriolis effect can be neglected relative to the nonlinear terms in the momentum equation. Therefore, to evaluate the basic dynamics of the system, let us

consider the shallow-water equations for the vertically averaged flow $(\overline{u},\overline{v})$ and surface elevation, η. Figure 8 indicates that the flow is quite barotropic and bottom friction seems to affect only the 1–5 m near the bottom, so the assumption of frictionless barotropic flow is not too unrealistic for scaling purposes. The momentum and continuity equations are:

$$\overbrace{\frac{\partial \overline{u}}{\partial t}}^{\substack{\mathrm{ACC}\\ U/T}} + \overbrace{\overline{u}\frac{\partial \overline{u}}{\partial x}+\overline{v}\frac{\partial \overline{u}}{\partial y}}^{\substack{\mathrm{NL}\\ U^2/L}} - \overbrace{f\overline{v}}^{\substack{\mathrm{COR}\\ fU}} + \overbrace{g\frac{\partial \eta}{\partial x}}^{\substack{\mathrm{PG}\\ g\Delta\eta/L}} = 0 \tag{1}$$

$$\frac{\partial \overline{v}}{\partial t}+\overline{u}\frac{\partial \overline{v}}{\partial x}+\overline{v}\frac{\partial \overline{v}}{\partial y}+f\overline{u}+g\frac{\partial \eta}{\partial y}=0 \tag{2}$$

$$\overbrace{\frac{\partial \eta}{\partial t}}^{\Delta\eta/T} + \overbrace{\frac{\partial}{\partial x}(\overline{u}D)+\frac{\partial}{\partial y}(\overline{v}D)}^{\mathrm{UH}/L} = 0\ ; \tag{3}$$

$$D = H+\eta,\ H \gg \eta.$$

Let us scale the equations to see which terms are more important than others (see scales on top of (1) and (3)). Given the observations during the storm and the general reef topography, the following typical scales can be assumed: velocity scale $U\sim 1\ \mathrm{ms}^{-1}$, horizontal length scale $L\sim 1\ \mathrm{km}=10^3\ \mathrm{m}$, elevation anomaly scale $\Delta\eta\sim 0.5$ m, time scale $T\sim 1$ day$\sim 10^5$ s, and depth scale $H\sim 100$ m. Therefore, in the momentum (Eqs. (1) and (2)), the terms from left to right have the following typical size (in meters per square second): the acceleration term (ACC) $\sim 10^{-5}$, the nonlinear terms (NL) $\sim 10^{-3}$, the Coriolis term (COR) $\sim 5\times 10^{-5}$, and the pressure gradient terms (PG) $\sim 5\times 10^{-3}$. Scaling of the continuity (Eq. (3)) shows that the time-dependent term is the smallest ($\sim 5\times 10^{-6}$), while the other terms have the size of ~0.1. The scaling shows that to first order, the time-dependent and the Coriolis acceleration terms can be neglected, so the leading terms imply the following balances (after rearranging the terms in the continuity equation, assuming that $H>>\eta$),

$$\overline{u}\frac{\partial \overline{u}}{\partial x}+\overline{v}\frac{\partial \overline{u}}{\partial y}=-g\frac{\partial \eta}{\partial x} \tag{4}$$

$$\overline{u}\frac{\partial \overline{v}}{\partial x}+\overline{v}\frac{\partial \overline{v}}{\partial y}=-g\frac{\partial \eta}{\partial y} \tag{5}$$

$$H\left(\frac{\partial \overline{u}}{\partial x}+\frac{\partial \overline{v}}{\partial y}\right)=-\left(\overline{u}\frac{\partial H}{\partial x}+\overline{v}\frac{\partial H}{\partial y}\right). \tag{6}$$

Therefore, the small-scale dynamics of the flow near the reef is dominated by two main characteristics. First, large topographic slopes (right-hand side of 6) will generate convergence and divergence in the currents (left-hand side of 6) when they approach the reef, as seen in the model simulations (Fig. 11). Second, changes in surface elevation are influenced by nonlinear dynamics (Eqs. 4 and 5). The scaling of Eqs. 4 and 5 imply that if NL~PG, the changes in surface elevation are proportional to the square of the velocity, $\Delta\eta\sim U^2/g$. Similar relation is also obtained in a steady, incompressible, irrotational one-dimensional flow obeying the Bernoulli's equation, $U^2/2+P/\rho+g\Delta\eta=B$, where P is pressure, ρ is density, and B the Bernoulli's constant (see for example, the increase in flow speed over a bump, Fig. 9.9 in Mellor 1996). The situation here is of course much more complicated, but the idea is similar, in the sense that when strong flows approach shallower reef area, the flow is intensified and pressure or water level may drop at the tip of the reef (at Nortek in our case) where the velocities are maximum; this may partly explain the spatial gradients in water levels. The impact of nonlinear effects on the dynamics becomes more pronounced with increasing velocity, such as in the case of the 17–21 October storm. When the flow speed is below some threshold (e.g., before or after the storm), the nonlinear terms become small and no significant spatial water levels are seen near the reef (Fig. 6c).

6 Discussion and conclusions

Studies of flow–topography interactions along the Belize coral reef in the western Caribbean Sea have been motivated by attempts to explain survival advantages that lead to multispecies spawning aggregations to occur at reefs with particular shapes (Heyman et al. 2005, 2008; Heyman and Kjerfve 2008; Kobara and Heyman 2008). Nevertheless, forcing mechanisms of flows and associated connectivity between spawning and nursing areas (Tang et al. 2006; Werner et al. 2007; Heyman et al. 2008) remain largely unknown. In particular, the relation between local flows on scales of a few meters to a few hundred meters and remote large-scale forcing by Caribbean mesoscale eddies and weather systems is not completely understood. There is evidence from regional models (grid size ~5 km) that offshore Caribbean eddies influence the near-reef flow (Ezer et al. 2005). A high-resolution reef model (grid size ~50 m) shows that variations in the large-scale flow and tidal currents are amplified by the shape of the reef, whereas mixing is induced by internal waves propagating toward the reef and breaking on its steep slopes (Ezer et al. 2011). The same high-resolution model is used here to study the so-called perfect storm case on 17–21 October 2009.

Oceanic measurements, taken on October 2009 near Gladden Spit reef as part of longer term monitoring campaign of the reef, revealed unusual changes that to our

knowledge have not been observed before or since then in this location. Water level rose by over 60 cm above normal (three times higher than maximum tides), and current speed larger than 1 ms^{-1} was observed (more than 6 standard deviations above the average flow speed). It was found that during this time several unusual events occurred simultaneously: The first event was a westward propagating cyclonic eddy that "crushed" into the coast and created a southward coastal flow that is much stronger than normal (Fig. 9). Large (~150–200 km in diameter) cyclonic eddies are commonly found in the Gulf of Honduras several times per year, and when propagating westward close enough to the reef, they have the potential to increase the southward coastal flow (Ezer et al. 2005). But this particular eddy in October 2009 got closer to the reef than others and occupied large portion of the Gulf of Honduras all the way to the Belize Reef. At the same time, a second event occurred, with the development of a short-lived local tropical storm with winds over 20 ms^{-1} (Figs. 3 and 4); this storm seems to be part of a chain of atmospheric disturbances along the western Caribbean Sea. Cyclonic atmospheric circulation at the center of this storm shows rotation scales of ~50–150 km in diameter; this wind pattern can contribute to the intensification of the southward flow. It is unclear if the two events are related, though one may speculate that unusual surface temperatures associated with Caribbean eddies may impact atmospheric instability, but this is beyond the scope of our study. The result of these two events was extreme southward flows over 1 ms^{-1}; a significant correlation was found between this local current and the large-scale geostrophic flow. The study shows how simultaneous events, including a Caribbean cyclonic eddy with flow of ~0.3 ms^{-1}, a local tropical storm with winds of ~20 ms^{-1}, and a Spring tide were combined to increase the normal mean southward coastal flow. While tidal amplitudes are relatively small in this region, they play a role in modulating the storm's impact, creating secondary peaks in the water level.

The fact that a relatively simple high-resolution reef model (Ezer et al. 2011) with an idealized topography (Fig. 1c) and idealized wind forcing (Fig. 10a) was able to simulate quite well the unusual currents (Fig. 10c) and water level changes (Fig. 12b) indicates that such a model is a useful tool to study the dynamic processes involved. In most cases, accurate simulations of storm surge due to on-shore wind-driven currents and waves, for example during hurricane Katrina (Wang and Oey 2008), are only possible with accurate wind data. However, in the study presented, water level rise was simulated quite well even without accurate wind forcing because the dynamics is different than classic wind-driven storm surge. Rather than local wind-driven currents, here the along shore coastal current is driven by the large-scale wind and eddy fields. When this coastal current reaches the shallower ridge and the curved small-scale reef topography, the flow is intensified and spatial water level variations are found upstream and downstream of the tip of the reef.

A simple scaling of the barotropic equations of motion indicates that with the steep slopes and strong curvatures of the reef (with length scales of 100 s of meters to a few kilometers), the nonlinear terms in the equations cannot be neglected. The nonlinearity of the system becomes more apparent as currents intensify, so that in the case of the "perfect storm" presented here, large changes of water level over a few kilometers of coast are not unexpected. While here the focus was on an event over a short period of a few days, further studies now underway focus on more detailed analysis of long-term observations and connectivity. In addition to the simple process study presented here, further modeling with nested models (e.g., Sheng and Tang 2004) should also be useful to connect small- and large-scale forcing.

The study presented here and other ongoing studies of the region will help assess the biological implications of flow–topography interactions near spawning aggregation sites. The biological implication from our case study on one reef is that other reefs that provide spawning aggregation sites and have similar small-scale curved shapes (Heyman et al. 2007; Kobara and Heyman 2008) should have similar dynamics that amplify currents and mixing.

Acknowledgments TE is partly supported by grants from NOAA. WH, CH, and BK were supported by grants from the Mellon Foundation, the World Bank, SDC, and the Conservation International's Marine Managed Area Science Program.

References

Ducet N, Le Tron PY, Reverdin G (2000) Global high-resolution mapping of ocean circulation from TOPEX/Poseidon and ERS-1 and -2. J Geophys Res 105:19477–19498

Ezer T (2005) Entrainment, diapycnal mixing and transport in three-dimensional bottom gravity current simulations using the Mellor-Yamada turbulence scheme. Ocean Model 9(2):151–168

Ezer T (2006) Topographic influence on overflow dynamics: idealized numerical simulations and the Faroe Bank Channel overflow. J Geophys Res 111(C02002). doi:10.1029/2005JC003195

Ezer T, Mellor GL (2004) A generalized coordinate ocean model and a comparison of the bottom boundary layer dynamics in terrain-following and in z-level grids. Ocean Model 6(3–4):379–403

Ezer T, Thattai DV, Kjerfve B, Heyman WD (2005) On the variability of the flow along the Meso-American Barrier Reef system: a numerical model study of the influence of the Caribbean current and eddies. Ocean Dyn 55:458–475

Ezer T, Heyman WD, Houser C, Kjerfve B (2011) Modeling and observations of high-frequency flow variability and internal waves at a Caribbean reef spawning aggregation site. Ocean Dyn 61(5):581–598

Heyman WD, Requena N (2002) Status of multi-species spawning aggregations in Belize. The Nature Conservancy. Arlington, Virginia. www.conserveonline.org

Heyman WD, Kjerfve B, Graham RT, Rhodes KL, Garbutt L (2005) Spawning aggregations of *Lutjanus cyanopterus* (Cuvier) on the Belize Barrier Reef over a 6 year period. J Fish Biol 67(1):83–101

Heyman WD, Ecochard JB, Biasi FB (2007) Low-cost bathymetric mapping for tropical marine conservation—a focus on reef fish spawning aggregation sites. Mar Geodesy 30(1):37–50

Heyman WD, Kjerfve B, Ezer T (2008) Mesoamerican reef spawning aggregations help maintain fish population: a review of connectivity research and priorities for science and management. In: Grober-Dunsmore R, Keller BD (Eds.) Caribbean connectivity: implications for marine protected area management pp. 150–169. Proc. Special Symposium, 9–11 November 2006, 59th Annual Meeting of the Gulf and Caribbean Fisheries Institute, Belize City, Belize. Marine Sanctuaries Conservation Series ONMS-08-07, NOAA, Silver Spring, MD

Heyman WD, Kjerfve B (2008) Characterization of transient multi-species reef fish spawning aggregations at Gladden Spit, Belize. Bull Mar Sci 83(3):531–551

Kobara S, Heyman WD (2008) Geomorphometric patterns of Nassau grouper (*Epinephelus striatus*) spawning aggregation sites in the Cayman Islands. Mar Geodesy 31:231–245

Lobel PS, Robinson AR (1986) Transport and entrapment of fish larvae by ocean mesoscale eddies and currents in Hawaiian waters. Deep-Sea Res 33(4):483–501

Mellor GL (1996) Introduction to physical oceanography. AIP Press, New York, p 260

Mellor GL, Hakkinen S, Ezer T, Patchen R (2002) A generalization of a sigma coordinate ocean model and an intercomparison of model vertical grids. In: Pinardi N, Woods JD (eds.) Ocean forecasting: conceptual basis and applications. Springer, Berlin, 55–72

Miloslavich P, Dı'az JM, Klein E, Alvarado JJ, Dı'az C et al (2010) Marine biodiversity in the Caribbean: regional estimates and distribution patterns. PLoS ONE 5(8):e11916. doi:10.1371/journal.pone.0011916

Oey L-Y, Ezer T, Wang D-P, Fan S-J, Yin X-Q (2006) Loop current warming by Hurricane Wilma. Geophys Res Let 33:L08613. doi:10.1029/2006GL025873

Oey L-Y, Ezer T, Wang D-P, Yin X-Q, Fan S-J (2007) Hurricane-induced motions and interaction with ocean currents. Cont Shelf Res 27:1249–1263

Sheng J, Tang L (2004) A two-way nested-grid ocean circulation model for the Meso-American Barrier Reef System. Ocean Dyn 54:232–242

Sheng J, Wang L, Andréfouët S, Hu C, Hatcher BG, Muller-Karger FE, Kjerfve B, Heyman WD, Yang B (2007) Upper ocean response of the Mesoamerican Barrier Reef System to Hurricane Mitch and coastal freshwater inputs: a study using sea-viewing wide field-of-view sensor (SeaWIFS) ocean color data and a nested-grid ocean circulation model. J Geophys Res 112(C07016). doi:10.1029/2006JC003900

Tang L, Sheng J, Hatcher BG, Sale PF (2006) Numerical study of circulation, dispersion, and hydrodynamic connectivity of surface waters on the Belize shelf. J Geophys Res 111(C01003). doi:10.1029/2005JC002930

Wang D-P, Oey L-Y (2008) Hindcast of waves and currents in hurricane Katrina. Bul Amer Met Soc 89(4):487–496

Werner FE, Cowen RK, Paris CB (2007) Coupled biological and physical models: present capabilities and necessary developments for future studies of population connectivity. Oceanography 20(3):54–69

Wing SR, Botsford LW, Ralston SV, Largier JL (1998) Meroplanktonic distribution and circulation in a coastal retention zone of the northern California upwelling system. Limn Oceanogr 43(7):1710–1721

Wright DJ, Heyman WD (2008) Introduction to the special issue: marine and coastal GIS for geomorphology, habitat mapping and marine reserves. Mar Geod 31:1–8